

CONTROLLED-DEPTH LASER CUTTING OF ALUMINUM SHEET FOR LAMINATED OBJECT MANUFACTURING

Gene Zak and Matthew Shiu

Centre for Automotive Materials and Manufacturing
Department of Mechanical Engineering, Queen's University, Kingston, ON, Canada K7L 3N6

Abstract

Replacing paper with metal in laminated object manufacturing would bring improvements in terms of part's longevity, and its mechanical and thermal properties. In fabricating laminated parts, a challenging step is blind cutting of the metal sheet. Challenges to overcome are (1) maintaining consistent depth of cut, (2) achieving good surface quality of the cut groove walls, and (3) minimizing the formation of recast. Results are presented of an experimental investigation into controlled-depth laser cutting of aluminum sheet. Thin (0.12-mm) aluminum sheet specimens were cut with a 10-W Nd:YLF laser while varying scan speed and laser power. To accurately observe the cut profiles, specimens were mounted in resin and sectioned. Special handling procedure was developed to handle thin sheet material while avoiding damage. Relationship between cut profile and process parameters was established and shown to conform to established theoretical models.

Introduction

Using laminations (i.e., material in sheet form) for layered manufacturing (LM) avoids phase transformations with attendant shrinkage (e.g., in powder sintering) and allows easy process scale-up. Number of researchers have explored this approach to fabrication of functional parts. Adams et al. [1] produced working tools from steel laminations 1-3 mm thick, but had resort to a finishing milling step to achieve acceptable surface quality. Himmer et al. [2] proposed to fabricate injection moulds by (1) joining flux-coated 2.5-mm-gauge aluminum through heat treatment near the flux melting temperature and (2) finish milling. Walczyk and Dolar [3] present results of tests on several epoxy and alumina-based adhesives used to bond aluminum laminations. All of these papers adopt the "cut-stack-bond" approach (Fig. 1a), meaning the process sequence is (1) cut out the desired part's profile at each layer's height; (2) assemble (stack) the profiles, and (3) bond them (mechanically with fasteners, adhesively, or by welding). The main disadvantage of the "cut-stack-bond" approach is the complexity of handling the cut-out profiles between the cutting and stacking steps, requiring indexing, transporting, and alignment. This complexity makes *automation* of the process highly impractical.

An alternative approach exists which is more amenable to automation. It is characterized by a "stack-bond-cut" sequence (Fig. 1b). This method has been applied in a commercial LM process, Laminated Object Manufacturing (LOM), but the sheet materials have been limited to paper or polymers [4]. Replacing soft materials with metals is a challenge, however, due to difficulties with "blind" cutting of metals (i.e., cutting only to the depth of the sheet's gauge).

This paper presents results of experimental investigation into controlled-depth blind laser cutting of aluminum sheet. Before presenting these results, background information on laser-machining of metals is provided.

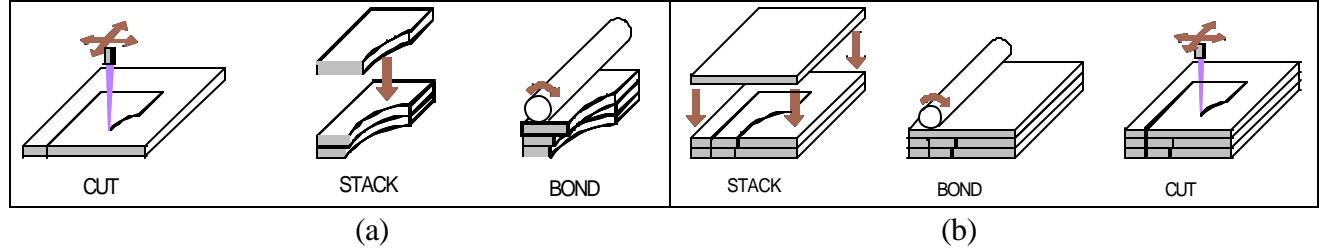


Figure 1. Two alternative sequences for producing laminated objects: (a) cut-stack-bond and (b) stack-bond-cut.

Laser Machining of Metals

Laser machining of metals is accomplished by achieving a sufficiently high power density (W/cm^2) at the focal point to melt or evaporate the material. The molten material is likely to resolidify, and thus, if most material in the groove is molten, it can produce poor-quality cut, making vaporization the preferred mode.

Through cutting vs. blind cutting: In through cutting, the molten and vaporized material can escape through the cut slot; on the other hand, in blind cutting, this material has to be evacuated through the groove's top opening. Pressurized gas is often used to assist cutting. With through cutting, the gas helps the debris to escape through the cut slot. The role of gas assist in blind cutting is not as significant (and potentially detrimental, pushing the material back into the groove). When cutting metal *laminations*, the situation more closely resembles blind cutting, since there is no escape route for the molten material and gases through the bottom of the cut. However, there is a difference as well since the groove is being cut not in a bulk material but through a thin sheet with a layer of adhesive below

Laser and optical system considerations: To achieve the high power density required for cutting aluminum ($10^6 - 10^9 \text{ W}/\text{cm}^2$) [5], we need to deliver the laser energy over a short time interval (on the order of tenth of nanoseconds) and into a very small area (diameter of 5-20 μm). Most suitable laser beam mode for metal machining is the fundamental (or Gaussian) mode TEM_{00} because it can be focused to a smallest spot and has the greatest depth of focus compared to other modes. The focal spot diameter is theoretically given by:

$$d = \frac{4 \lambda f}{\pi D} \quad (1)$$

where λ is laser light wavelength, f is the focal length of the focusing lens, and D is the diameter of the incident beam. Depth of focus is another important factor to be aware of. It is defined as the distance within which the power density is greater than 90% of its peak value at the focal point. It can be calculated by:

$$Z = \frac{8 \lambda f^2}{\pi D^2} \quad (2)$$

If Z were too small, even slight surface irregularities and misalignment of specimen surface and X-Y translation plane may cause significant variations in power density. On the other hand, if Z were to be made larger by increasing f or decreasing D , it would also increase the focal spot diameter (Eq. 1), and therefore decrease power density. Thus, given the initial beam diameter and laser wavelength, the appropriate choice of beam expansion ratio (affecting D) and focal length involves a trade-off between minimizing the focal spot diameter (d) and maximizing the depth of focus (Z).

Laser grooving theoretical models: While much research has been conducted in the area of through cutting of metals [6, 7], the more relevant subject for our work is that of blind cutting (or *laser grooving*). For example, Modest [8] developed a 3-D conduction model to predict the transient effects in laser machining of ablating/decomposing materials. The model predicts not only the depths but also the shape of a developing groove formed by ablation of material (e.g., aluminum). Chryssoulouris [9] developed a simpler closed-form generalized model to address cutting, drilling, and grooving processes. The model is derived by considering the heat-transfer balance at the constant erosion front produced by the moving laser beam. It predicts the groove depth as:

$$L_d = \frac{2aP}{\rho^{1/2} r V d (C_p (T_s - T_o) + L)} \quad (3)$$

where a is the material absorptivity ($0 < a < 1$), P is the incident laser power, ρ is the material density, V is the beam scanning speed, d is the focal spot diameter, C_p is the specific and L is the latent heat, and T_s and T_o are the vaporization and room temperatures, respectively. The relationship implies that the groove depth L_d is directly proportional to the laser power and inversely proportional to the scanning speed. The model assumes that the material is isotropic and its properties are constant; the material changes phase from solid to vapour in one step at a single evaporation temperature; the evaporated/ejected material does not interfere with the beam reaching the erosion front; multiple reflections of the beam within the groove are neglected; and material is removed by vaporization (sublimation cutting).

Laser cutting experiments

Objectives: Experiments were conducted with the overall objective of finding suitable processing parameters for controlled-depth cutting of the aluminum sheet material in laminated object manufacturing. The primary controllable process parameters are laser power and scan speed. The primary measured characteristic is the groove depth. The primary interest in groove depth is due to the need to cut the sheet laminations precisely to the depth of one sheet without significant damage to the underlying stack. A second objective was to determine the effect of changing the material being cut from a (relatively) thick aluminum plate (3.2 mm) to a stack of thin laminated sheets (sheet thickness 0.12 mm). Laser grooving is normally performed on relatively thick material and theoretical predictions would normally also be made for such materials. On the other hand, the material to be cut in our case consists of a sandwich of polymeric adhesive and aluminum sheet. Aluminum is an excellent heat conductor (thermal conductivity 210 W/m C) while a typical adhesive acts as an insulator, with very low conductivity (0.2-0.5 W/m C). Thus, the solid plate represents a “reference” case while the laminated sheet specimens approximates the special material combination to be encountered in the laminated fabrication process.

Specimen Preparation: Two types of specimens were used: solid plates or laminated sheets. The plates were prepared by cutting 2"×1/8" (50.8 mm×3.2 mm) aluminum alloy bar stock (ASTM B221 6061 T6511) into 95 mm lengths. These plates were used either directly or as supports for three laminated sheets bonded to them. The latter were cut from a rolled aluminum sheet stock (6061, 0.05" or 0.12 mm gauge) into 90 mm by 20 mm strips. To bond the sheet strips to the support plates, (1) the plates were sanded, (2) plate and sheet surfaces were cleaned by chemical etching, (3) adhesive was applied to the sheets, and (4) using the heat sealer, the strips were bonded one on top of another starting with the support plate. To bond the sheets, a film adhesive was used (Scotch 467MP from 3M consisting of 200MP high-performance acrylic adhesive (50 microns) with polycoated Kraft paper liner).

Laser Machining Equipment: The experimental setup consisted of a laser light source, a beam delivery system, and a motion system¹. The platform carrying the specimen moved in X-Y plane (with accuracy of ±1 μm) while the optical system remained stationary. The light source was a GSI Lumonics Sigma-400 diode-pumped Nd:YLF laser operating at a wavelength of 1054 nm (near infrared), capable of up to 12W average power and (Q-switched) pulse frequency up to 20 kHz.

The optical path from the laser to the specimen surface consisted of five-time beam expander/collimator, three mirrors, and a 55-mm apochromat triplet lens. Given the light wavelength, initial beam diameter (1.3 mm), beam expansion ratio, and the focal length, the theoretical focal spot diameter is estimated by Eq. (1) to be 11.3 μm. The depth of focus is estimated using Eq. (2) to be only 112 μm, which implies that care must be taken to make sure the specimen surface is parallel with the plane of X-Y motion and that the beam is properly focused. Assuming actual focal spot diameter to be approximately 15 μm (larger diameter is expected due to optical aberrations of the non-ideal focusing lens), the power density at the specimen's surface during a single pulse can be estimated to range from 2.3 to 6.8×10⁹ W/cm² for laser power outputs of 4W to 12W and pulse frequency of 10 kHz used in the experiments. Therefore, our experimental setup was capable of producing sufficient power density to vaporize the aluminum.

Test Procedure: For each specimen, four groups of seven parallel 3.7-cm lines were scanned, with two groups scanned for each power setting (Figure 2). The scan directions in the two groups were reversed with the intention to ascertain absence of any directional effects. (Due to experimental error, for Set 1, both sets of lines for 4 and 7W were drawn in the same direction. Since no significant difference between directions was observed for the two higher powers of Set 1, this error is not expected to affect the results.) Within each group, the scan speed increased from right to left as viewed in the figure, from 1500 to 4500 in 500 mm/min increments. Four power settings were used: 4, 7, 10, and 12W, all at pulse frequency of 10 kHz and pulse duration of 100 ns.

Data Collection: After experimenting with other examination techniques (SEM and vertical scanning interferometry, i.e., profilometry), it was found that the only reliable way to obtain the desired information was via metallography. The difficulties with examining the specimens are caused by the narrow width of the grooves (as little as 15 μm), their fragility, high height to width ratio (up to 8 to 1), and presence of recast and other debris within the groove cut obscuring the groove bottom from non-destructive optical

¹ Experiments were conducted at the Laser Micromachining Facility, Toronto, Ontario.

examination. The drawbacks of the metallographic examination are that it is destructive and labour-intensive.

To make sure that the fragile sheets are completely immobilized, a two-stage mounting process was developed. In the first stage, a 25-mm segment of the support plate with the sheet layers attached was cut away from each side of the specimen (see Figure 2). Each piece was placed in a rectangular rubber mould (85L × 53W × 30H mm), and set in epoxy (Araldite GY502). This epoxy block was cut into two pieces, each containing one line group, and, in the second mounting stage, these two pieces were mounted in epoxy within a one-inch diameter cylindrical mould. After polishing to 0.5 μm finish, gray-scale images of sections (256-level, 975×975 pixels) were captured through an optical microscope and used subsequently to measure the groove cross-section features with a resolution of 0.25 μm/pixel.

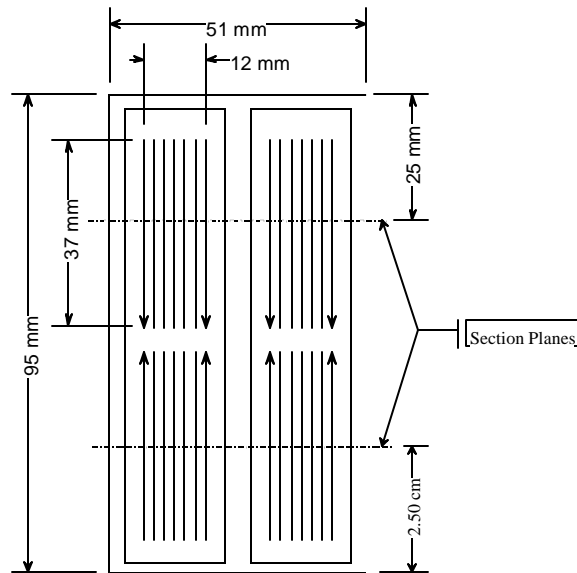


Figure 2. Geometry of specimens and line scans (same line pattern was used for all specimens).

Results and Discussion

The observed features of groove cross-sections were groove depth (L_d) and recast area fraction (A_r). The amount of recast within the groove indicates how successful the laser was in severing the sheet. A_r is defined as a percent fraction of profile cross-section area occupied by recast. The areas were measured with the aid of Scion Image image-processing software.

Set 1: Solid-plate Specimens: Figure 3 shows two examples of groove cross-sections, one with significant recast present and another showing a successful (clean) groove. Both figures show upward molten material flow pattern which developed as the vaporized and molten metal escaped vertically. Recast occurs when molten and vaporized metal resolidifies upon coming in contact with the relatively cool walls of the groove. Under certain process conditions, there is enough resolidification to form a “bridge” across the groove.

Figure 4(a) shows the groove depths (L_{dl}) averaged from two observations. As expected, the groove depth decreases with scan speed and increases with laser power. Also shown on the same plot are the results of fitting the model in Eq. (3) to our data. The parameter values used for the model were:

$r = 2700 \text{ kg/m}^3$, $d = 30 \text{ }\mu\text{m}$, $C_p = 896 \text{ J/kgC}$, latent heats of fusion 395 kJ/kg and vaporization 10.5 MJ/kg , $T_s = 2467^\circ\text{C}$. The model curves were “fitted” by adjusting the absorptivity value (a). The resultant plots are for $a = 0.48$. Even though this value is higher than the rated absorptivity of aluminum (0.2-0.25), it is well-known that a rises at elevated temperatures [5]. An excellent fit was obtained for all but the lowest power setting. It is possible that the model fails at this setting since it assumes that the material removed from the groove is completely vaporized (i.e., all absorbed incident energy is used to vaporize the groove material). At the lowest power, this assumption may not be valid.

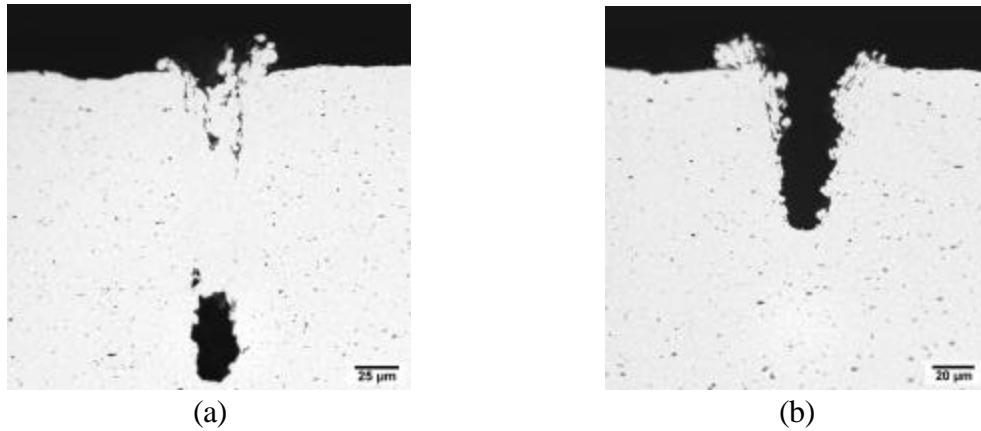


Figure 3. Examples of groove cross-sections for solid-plate specimens: (a) recast-filled groove (12W, 2000 mm/min); (b) clean groove (12W, 4500 mm/min).

Figure 4(b) shows how recast area fraction (averaged from two observations) decreases linearly with scanning speed. The value falls quickly from nearly 100% at 1500 mm/min to, on average, about 30% for 4500 mm/min. There is no significant dependence on the laser power.

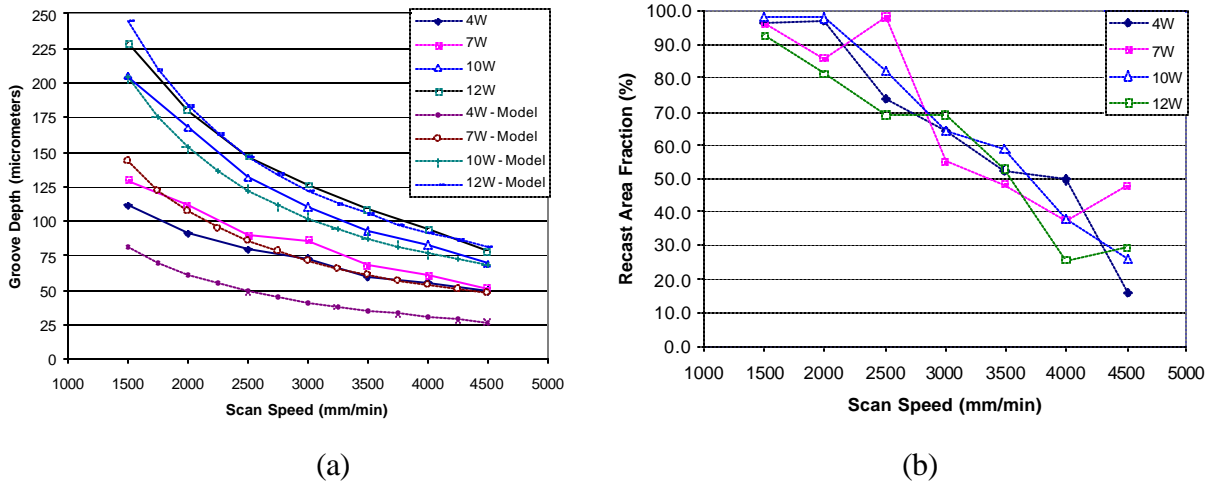


Figure 4. (a) Groove depths (experiment and model) and (b) recast area fraction for solid-plate specimens as a function of scan speed.

Set 2: Laminated-sheet Specimens: For laminated-sheet specimens, some combinations of speed and power resulted in successful through cutting of the aluminum sheet (Fig. 5a) while others produced grooves, similar to the solid-plate specimens (Fig. 5b). The trends for the groove depth values (L_{d2})

shown in Figure 6(a) are similar to those observed for the solid-plate specimens except for the upper limit of 120 μm (sheet thickness).

Recast area fraction for laminated-sheet specimen (A_{r2}) displays some of the trends of the solid-plate specimens, but also has some different features (Fig. 6b). In a trend similar to that for the solid-plate specimens, for speeds above 2000 mm/min, the recast area decreases with speed. One important difference, however, is a significant decrease in recast formation at 1500 mm/min for the two highest powers (10 and 12W). These are also the powers and speeds at which a through-cut was observed (see Fig. 5a). It is conjectured that at these higher powers and lower speeds, sufficient energy is delivered through the cut groove to the adhesive below to increase the pressure from vaporized material to the point where the material is removed from the groove before it is able to resolidify.

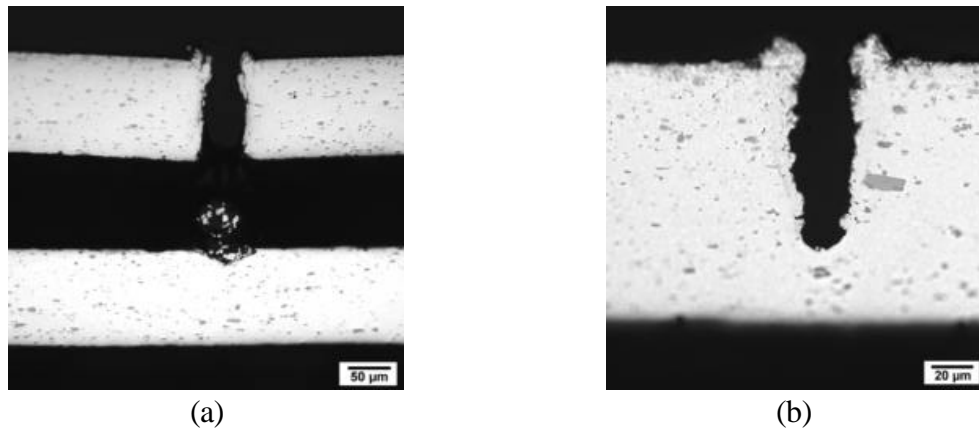


Figure 5. Examples of groove cross-sections for laminated-sheet specimens: (a) through-cut sheet (12W, 1500 mm/min); (b) recast-free groove (12W, 4500 mm/min).

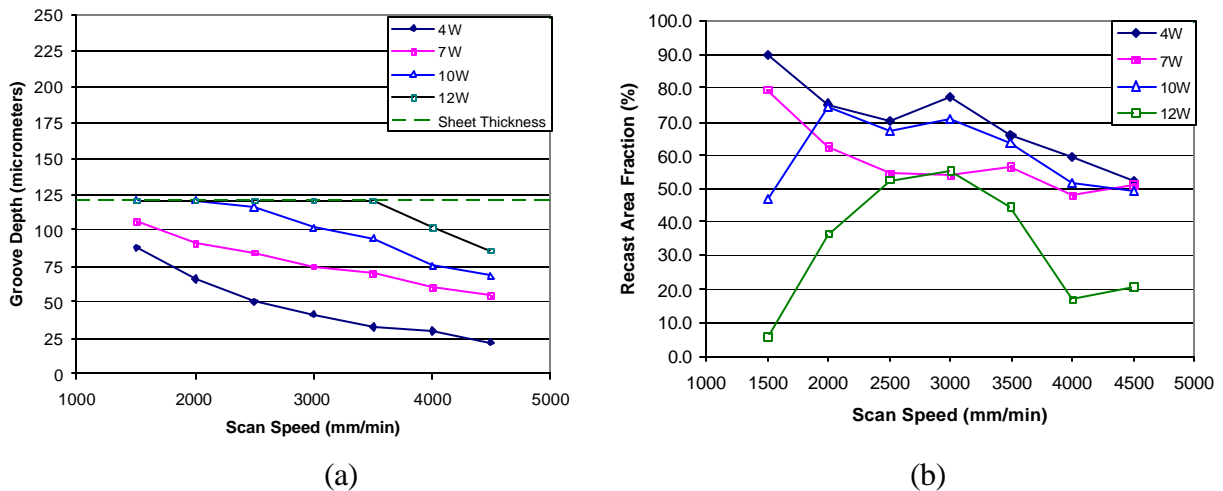


Figure 6. Groove depths (a) and recast area fraction (b) for laminated-sheet specimens as a function of scan speed.

Comparison of Set 1 and 2 Results: Figure 7 shows the ratio of groove depths for laminated sheet over those for solid plate: $y_d = L_{d2}/L_{d1}$. For example, values of y_d less than one would indicate that, for equivalent power and speed parameters, shallower grooves were produced in the laminated-sheet

specimens. It is interesting to observe that there is a consistent decline in this ratio with speed for the lowest power (4W), from 0.79 to 0.44, but, for all other (higher) powers, the ratio increases linearly with speed, reaching nearly unity at the highest speeds. Also, at the lowest speeds (1500 and 2000 mm/min), laser power does not appear to affect the y_d ratio.

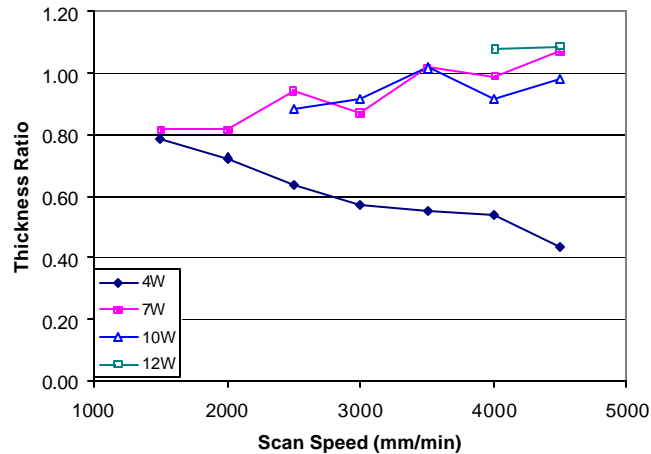


Figure 7. Ratio of groove depths for laminated sheet vs. solid plate ($y_d = L_{d2}/L_{d1}$).

Conclusions

From laser-cutting experiments on solid aluminum plates and laminated sheets, the relationship between the process parameters (scan speed and laser power) and groove depth was determined and found to agree well with the established theory. Additionally, a consistent relationship between the groove depths in the solid plate and in the laminated sheets was found. A novel method of metallographic examination of fragile laminated-sheet specimens was developed. Process parameter settings were found which resulted in recast-free through cut of uppermost sheet without significant damage to underlying stack.

Acknowledgements

We gratefully acknowledge the financial support of Centre for Automotive Materials and Manufacturing and Canada Foundation for Innovation. Our appreciation to Laser Micromachining Facility, Toronto, Canada, and to Marc Nantel for his advice. We also wish to express our thanks for assistance with specimen sectioning to Ms. W. Clapp and for microscope imaging to Ms. S. Hinchcliffe, both of Alcan Research Centre Labs.

References

- [1] C. Adams, B. Bryden, D. Wimpenny, "Rapid laminated tooling – making the technology work," 8th *European Conf. Rapid Prototyping and Manufacturing*, Nottingham, UK, Jul 1999, pp. 511-527.
- [2] T. Himmer, T. Nakagawa, M. Anzai, "Lamination of metal sheets," *Computers in Industry*, V. 39, 1999, pp. 27-33.

-
- [3] D. Walczyk, N. Y. Dolar, "Bonding methods for laminated tooling," *Solid Freeform Fabrication Symp.*, Austin, TX, Aug 1997, pp. 211-221.
- [4] M. Feygin, "Apparatus and method for forming an integral object from laminations," US Patent No. 4,752,352.
- [5] J. F. Ready, **LIA Handbook of Laser Materials Processing**, Laser Institute of America, Magnolia Pub., 2001.
- [6] K. A. Bunting and G. Cornfield, "Toward a General Theory of Cutting: A relationship Between the Incident Power Density and the Cut Speed", *Transactions of ASME-Journal of Heat Transfer*, 1975, pp. 116-122.
- [7] H. Kaebernick, D. Bicleanu, and M. Brandt, "Theoretical and Experimental Investigation of Pulsed Laser Cutting", *Annals of the CIRP*, V. 48, N. 1, 1999.
- [8] M. F. Modest, "Three-dimensional, transient model for laser machining of ablating/decomposing materials", *Int. J. Heat Mass Transfer*, V. 39, N. 2, 1996, pp.221-234.
- [9] G. Chryssolouris, **Laser Machining-Theory and Practice**, Springer-Verlag, 1991.